Hydraulic Erosion in Tailings Dam Breach Analysis

H. Joanna Chen
WSP Golder, Calgary, Alberta, Canada

ABSTRACT: Understanding of tailings hydraulic erosion characteristics and estimates of eroded tailings volume by supernatant pond stored are critical in a tailings storage facility breach analysis. In this paper, an erosion-based methodology is proposed to numerically simulate the hydraulic erosion process on tailings. Tailings eroded and carried by discharged water during a breach were modelled using computer program MADflow as non-Newtonian fluids. The flow mixture of water and eroded tailings was simulated with varying solids concentrations and the resulting outflow hydrograph contains time-dependent solids concentration during the erosion process. The proposed methodology was validated with a flume experiment.

A case study example was performed to illustrate the tailings hydraulic erosion process. Parametric analysis shows that the average volumetric solids concentration of outflow mixture of water and eroded tailings from the hydraulic erosion does not exceed 30% for the probable range of parameters analyzed. The eroded tailings volume is not directly connected to the storage volume of deposited tailings. Geotechnical properties and integrity of the deposited tailings play a significant role in erodibility and influence the volume of eroded tailings. The volume of eroded tailings shows logarithmical trend with initial pond volume.

1 INTRODUCTION

The Canadian Dam Association (CDA) Technical Bulletin Tailings Dam Breach Analysis (CDA 2021) presents conceptual cases for tailings dam breach analysis by considering two main components, including whether a supernatant pond in a tailings storage facility could release in a breach event, and whether liquefaction-induced flowable tailings could occur due to various triggering mechanisms including the breach itself. The processes of tailings outflow are complex and can be understood as two processes for tailings dam breach analysis purposes. Process I represents the discharge of the supernatant pond that carries eroded tailings and dam-fill materials, where eroded dam-fill volume directly depends on the size of the breach and, in many cases, has a much smaller volume than the other components (e.g. tailings and supernatant water) in the breach outflow volume. Process II represents the discharge of flowable tailings due to tailings liquefaction or progressive slumping of unsupported tailings.

For Process I, understanding of the tailings hydraulic erosion characteristics and estimates of eroded tailings volume by supernatant pond are critical when a supernatant pond exists and could be released. Sediment erosion studies were typically focused on natural water floods that erode and transport sediments (e.g. Temple 1985; O'Brien 1986; Hanson 1989, 1990; García et al. 2008; Briaud et al. 2017). For tailings erosion volume estimate in Process I, Fontaine and Martin (2015) proposed a conceptual method where the eroded tailings volume considers the supernatant pond volume, tailings density and degree of saturation, and the resulting outflow mixture of water and eroded tailings is related to a pre-defined solids content.

In this paper, an erosion-based methodology implemented with hydraulic erosion mechanism was proposed to numerically simulate the tailings hydraulic erosion process and estimate the volume of eroded tailings using computer program MADflow. The properties and integrity of the deposited tailings and the amount of available pond water are essential to the volume of eroded tailings. The proposed methodology was validated with a flume experiment and its application was illustrated with a case study example.

2 HYDRAULIC EROSION MECHANISM

The process of hydraulic soil erosion is the result of interaction between three main components: the erodible material, the eroding fluid (in most cases water), and the geometry of the obstacle impacting the flow. The fluid generates the load and the erodible material provides resistance in this process while the obstacle induces the disturbance (Briaud et al. 2017). In the study of erodibility of soils in earthen channels, hydraulic erosion mechanism by Hanson (1989) proposed that the rate of erosion (ε_r) is proportional to the effective hydraulic shear stress (τ_e) when τ_e exceeds the critical shear stress (τ_c) to initiate surface erosion or detachment of the sediments.

$$\varepsilon_r = k_d \cdot (\tau_e - \tau_c) \tag{1}$$

where k_d is the erodibility or detachment coefficient, and τ_e can be calculated by:

$$\tau_e = \gamma D S' (n_s/n)^2 \tag{2}$$

where γ is the unit weight of water, D is the flow depth, S' is the energy slope, n_s is the Manning's soil grain roughness for bare earth channels, and $n_s = 0.0156$ has been used in many studies of the erodibility of fine-grained soils (e.g. Temple 1985; Hanson 1989, 1990). The Manning's roughness coefficient (n) for the total flow can be calculated by:

$$n = D^{2/3} S'^{1/2} / u \tag{3}$$

where u is the flow mean velocity.

The critical shear stress (τ_c) and the erodibility coefficient (k_d) can be measured using the Jet Erosion Test, open channel flume experiments and laboratory erosion function apparatus. Briaud et al. (2017) presented soil erodibility classification charts and erosion threshold charts for different soil types based on a database of eighty-four erosion function apparatus tests with soil types ranging from coarse-grained materials to fine-grained soils, where the erosion rate is categorized based on shear rate and velocity. In addition, the charts correlate soil erodibility parameters to the geotechnical properties of soils, where the critical shear stress (τ_c) can be calculated by:

$$\tau_c = (\rho g n^2 v_c^2) / (H)^{0.33} \tag{4}$$

where ρ is the density of water, H is the water depth, and v_c is the critical flow velocity. Both v_c and τ_c are related to the mean grain size d_{50} with different correlations for coarse-grained and fine-grained soils.

3 MODEL VALIDATION

3.1 *Model Setup*

The model validation was setup referencing to the open channel erosion experiment conducted by Hanson and Cook (2004). The open channel erosion test was constructed in a flume, consisting of a 1.8 m wide by 29 m long flume with 2.4 m sidewalls. A flat-bottomed channel bed of 1.8 m wide and 21 m long was constructed in the flume. Soils (CL in the ASTM classification) were placed in the flume at a 3% slope in 15 cm loose lifts and compacted with four passes of a vibratory roller compactor, two passes without vibration, and two with vibration.

3.2 *Measurement from Flume Experiment*

Water flow was introduced in the flume. Readings of water surface and bed surface were taken along the centerline of the channel for a 6 m long testing section to determine erosion. The discharge was set at 0.71 m^3/s for duration of 1089 minutes. At the end of 1089 minutes, an average erosion depth of 11.1 cm was measured along the testing section.

3.3 *Measurement from Jet Test*

The submerged jet test apparatus provided a method of measuring the resistance in a localized area of the channel soil bed. A total of three measurements were carried out on the soil bed beyond the testing section. The erodibility coefficient (k_d) and critical shear stress (τ_c) were measured from the jet tests at the three locations as listed in Table 1.

It is noted that, among the three jet tests, the measured k_d at locations #1 and #3 are almost identical, while k_d measured at location #2 doubles its value compared to the measurements at locations #1 and #3. The measurements suggest that local area around location #2 is less resistant which may be caused by less soil contact pressure by the compactor, and/or having soil cluster with different properties (e.g. water content, grain size distribution, plasticity parameters, etc.). Heterogeneity is not uncommon in soil compaction. To have an appreciation of how representative of the measurements taken from the jet tests, the measured parameters were averaged for sensitivity analysis in the modelling.

Table 1. Measurements from jet tests

Test Location	τ_c (Pa)	k_d (cm^3/N-s)
#1	0.463	0.065
#2	0.913	0.135
#3	1.929	0.066
Average #1, #3	1.196	0.066

* τ_c and k_d were measured at three locations beyond the flume erosion testing section.

3.4 *Hydraulic Erosion Modeling*

The hydraulic erosion mechanism by water flow was integrated in MADflow. The program is capable of incorporating irregular three-dimensional terrain, entrainment of material from the flow base, temporal and spatial variation of yield stress and viscosity and specific weight of the flow mixture. It is equipped with commonly used rheological constitutive relationships and completed validations on various flume experiments for tailings flow, slurry flow, and granular flow for different rheological models, as well as field case history matching on historical tailings dam breach failures. The simulations provide a good match with the available laboratory and field observations (e.g., Chen and Lee 2000, 2002; Chen et al. 2006, 2019; Chen and Becker 2014; Chen and Cunning 2021; Ghahramani et al. 2022).

In the hydraulic erosion modelling, the resistance parameters measured at the three locations of the channel bed beyond the flume testing section as well as their average values were applied to the flume experiment numerical modeling. For each modelling, each set of the k_d and τ_c was assigned to the flume experiment soil beds.

The results of hydraulic erosion modelling are summarized in Table 2 and Figure 1. The calculated average erosion depth at the end of 1089 minutes using the parameters measured at locations #1 and #3 as well as their average values match well with the flume experiment measurements, and the difference is within 3%. The calculated average erosion depth using the parameters measured at location #2 has a greater erosion depth than the flume measurement. Measurements at locations #1 and #3 are more representative for the soil bed conditions along the flume testing section.

Table 2. Comparison of erosion depth between flume measurement and modelling.

τ_c and k_d measured from jet tests at location*	Modelled average erosion depth using τ_c and k_d from jet tests (cm)	Difference between modelling and measurement from flume experiment
#1	11.4	2.9%
#2	23.3	110.1%
#3	11.0	-1.2%
Average #1, #3	11.2	0.8%

* The above τ_c and k_d were used in erosion modelling of the flume experiment. An average erosion depth of 11.1 cm was measured along the flume testing section. Parameters measured at locations #1 and #3 are representative for the soil bed conditions of the flume erosion experiment.

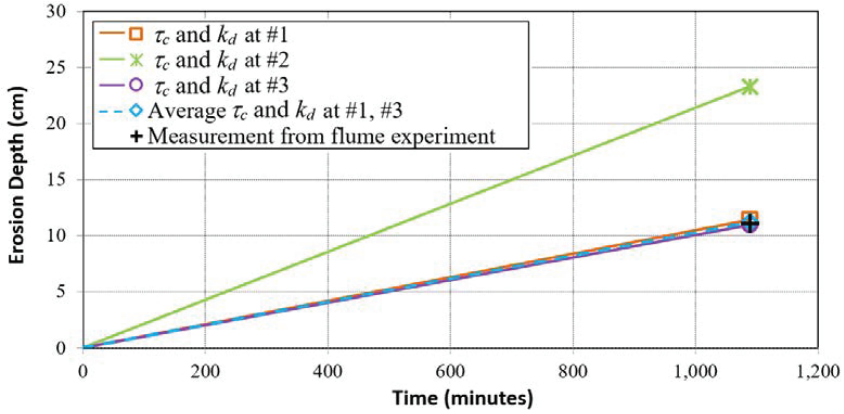

Figure 1: Modelled average erosion depth with time for duration of 1089 minutes, and erosion depth comparison between flume experiment measurement and numerical modelling at the end of 1089 minutes; using parameters measured at locations #1, #2, #3 and the average value.

4 ANALYSIS ILLUSTRATED BY AN EXAMPLE

4.1 *Site Conditions*

A tailings storage facility is located in a valley impoundment. The impounded tailings were deposited from spigotting and are contained by surrounding natural ridges of the valley and a cross-valley embankment dam. The dam was constructed by compacting successive layers of suitable soils using centerline method-of-construction. No tailings deposition has occurred in a decade. The previously deposited impounded tailings are currently covered with approximately 10 m high water in the facility.

The tailings storage volume is about 9.2 million m^3. The volumetric solids concentration of the deposited tailings approximates 43%, the dynamic Bingham yield stress and viscosity for the tailings samples are 15 Pa and 10 Pa·s respectively, and unit weight is 15.5 kN/m^3. The supernatant pond volume is approximately 3 million m^3.

The saturated tailings mainly consist of fine-grained sand and non-plastic silt with some clay. A screening-level tailings liquefaction assessment performed using the available piezo cone penetration test data shows that the tailings are susceptible to liquefication. One of the critical failure scenarios is a slope failure induced by seismic events. It is assumed that, in a hypothetical extreme earthquake event, a segment of the embankment dam could breach in a deep-seated failure mode. The assumed breach height and average breach width are approximately 40 m and 245 m, respectively.

4.2 *Hydraulic Erosion of Tailings*

The study focused on discharge of the supernatant pond carrying eroded tailings, where the eroded dam-fill material was not included given its negligible volume compared to the eroded tailings and supernatant pond volumes. When the supernatant pond propagated towards the breach opening, the tailings eroded is carried by discharge of the pond water stored in the facility. The rheological properties of the eroded tailings interacting and mixing with water, including the yield stress, viscosity and specific weight of the flow mixture, are calculated in each time step. Accordingly, the simulated flow mixture consisting of water and eroded tailings has varying solids concentration. The resulting outflow hydrograph contains time-dependent solids concentration of the mixture of water and tailings during the erosion process. The erodibility coefficient of 150 cm^3/(N-s) or 0.15 m^3/(kN-s) and critical shear stress of 0.1 Pa were conservatively assigned in the modelling.

A plan view of initial tailings depth distribution in the storage facility prior to breaching is shown in Figure 2 (A). As a comparison, the eroded tailings depth distribution at 8 minutes after breaching is shown in Figure 2 (B).

Figure 3 provides snapshots of the simulated tailings hydraulic erosion process along Section A-A' where the embankment dam breached in a deep-seated failure mode.

Figure 4 shows the time-dependent volumetric solids concentration of the mixture of water and eroded tailings changing with time when the tailings are eroded and carried by the pond water.

These figures show that, at the early stage, water outflow dominants with less erosion of tailings, followed with enhanced erosion of tailings with time. The volume of water and eroded tailings mixture as well as its volumetric solids concentration increase with time when water is available to allow for tailings erosion. Discharge of the pond continues to erode tailings in the impoundment until the pond is depleted. When most water flows away while carrying eroded tailings, the solids concentration and the volume of the outflow mixture of water and eroded tailings approach constant, suggesting the near completion of the hydraulic erosion process.

In addition, tailings in the vicinity of the breach opening are heavily eroded with deep scour by hydrodynamic forces, whilst tailings located in far field from the breach opening has much less involvement in the hydraulic erosion process.

The total volume of water and eroded tailings mixture from the hydraulic erosion is approximately 4.6 million m^3, including eroded tailings volume of approximately 1.6 million m^3. The average volumetric solids concentration of the total outflow mixture of water and eroded tailings is approximately 15%.

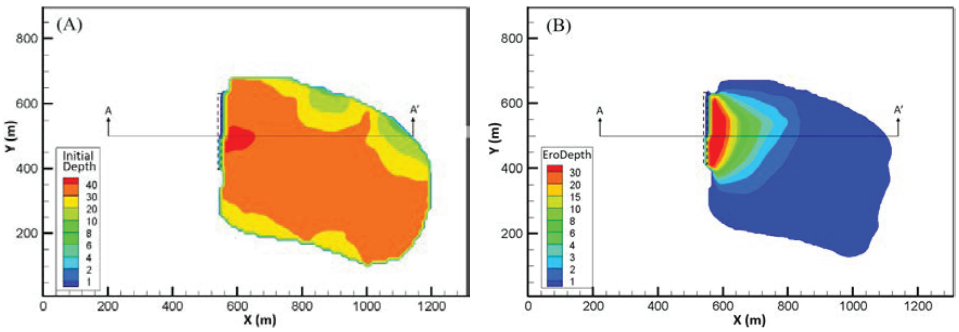

Figure 2: (A) Initial tailings depth distribution in the storage facility prior to tailings hydraulic erosion; (B) eroded tailings depth distribution at 8 minutes (section view along Section A-A' in Figure 3). Deashed lines illustrate breach location and breach width at the embankment dam crest.

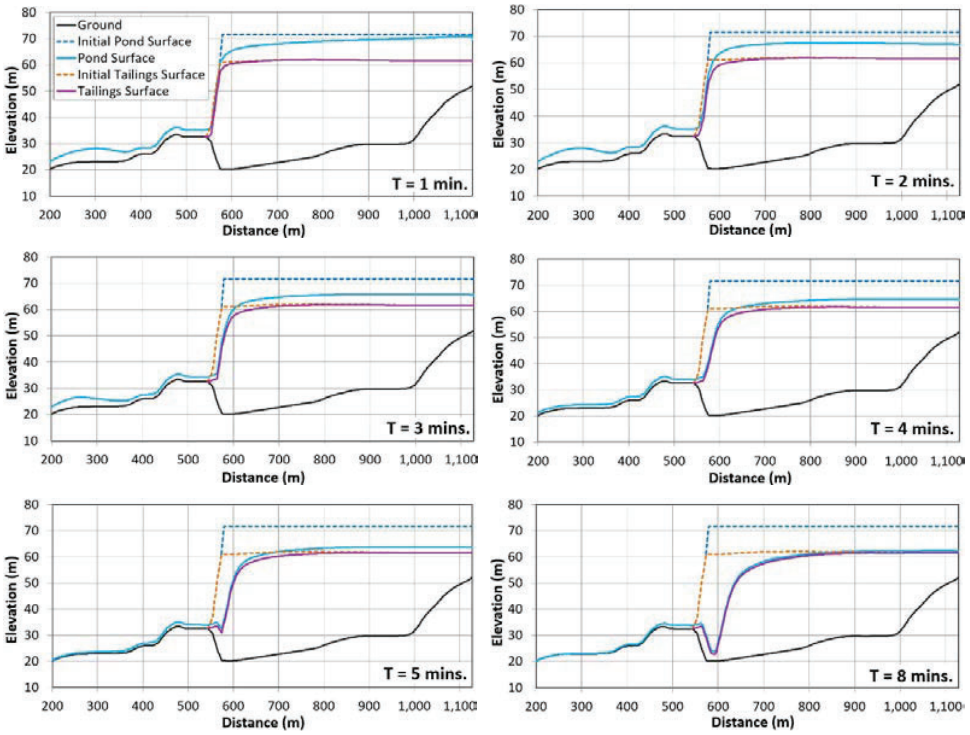

Figure 3: Snapshots of simulated tailings hydraulic erosion process along Section A-A' where the embankment dam breached.

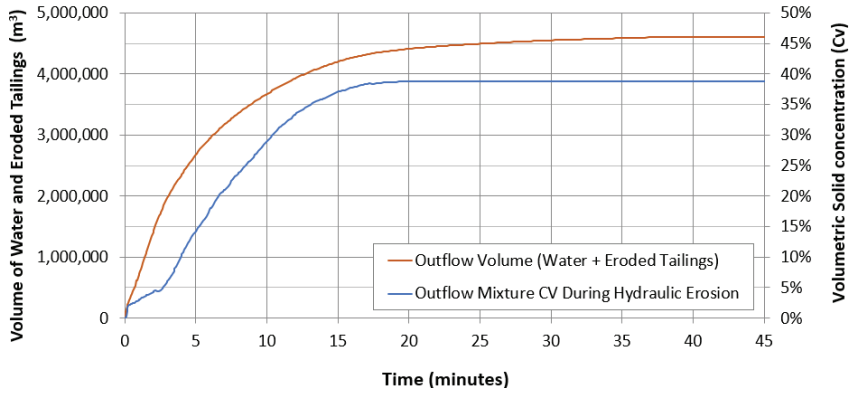

Figure 4: Changes of volume and volumetric solids concentration of flow mixture of water and eroded tailings with time.

4.3 *Parametric Study*

Erodibility coefficient and initial pond volume are the two main components that influence the volume of eroded tailings. Once effective hydraulic shear stress exceeds the critical shear stress, erosion of sediment occurs. To have an appreciation of how these two key parameters influence the volume of eroded tailings and the average volumetric solids concentration of the total outflow mixture of water and eroded tailings, parametric analysis was conducted using probable range of erodibility coefficient and varied pond volume.

Erodibility coefficient (k_d) and critical shear stress (τ_c) are related to soil properties and integrity. For cohesive sediments, k_d typically ranges from 2.5 cm^3/N-s to 30 cm^3/N-s (e.g. Wu 2013). For sand, silt and clayey soil with low compaction, k_d can range from 0.2 cm^3/N-s up to 200 cm^3/N-s (e.g. Hanson et al. 2011, Briaud et al. 2017). k_d of 200 cm^3/N-s may represent the probable upper bound of erodibility coefficient based on the currently available measurements, though they are not a replacement for site-specific erosion testing which represents the best solution if budget and schedule of a project allow for it.

Parametric analysis was focused on the erodibility coefficient and initial pond volume prior to tailings hydraulic erosion, where k_d varied from 10 cm^3/N-s (or 0.01 m^3/kN-s) for typical mid-value of cohesive sediments to 200 cm^3/N-s (or 0.2 m^3/kN-s) for probable upper bound value of non-cohesive soils. The critical shear stress was conservatively taken as 0.1 Pa to initiate erosion. Initial pond volume varied from approximately 1 million m^3 to 5.9 million m^3 above tailings by adjusting the pond water level. The tailings storage volume is about 9.2 million m^3. The breach geometry remains the same for each analysis scenario.

4.4 *Parametric Analysis Results*

The analysis results are provided in Figure 5, where the solid lines represent the volume of eroded tailings, the dashed lines represent the average volumetric solids concentration of the total outflow mixture of water and eroded tailings after completion of hydraulic erosion, and the same colorway represents the same analysis scenario.

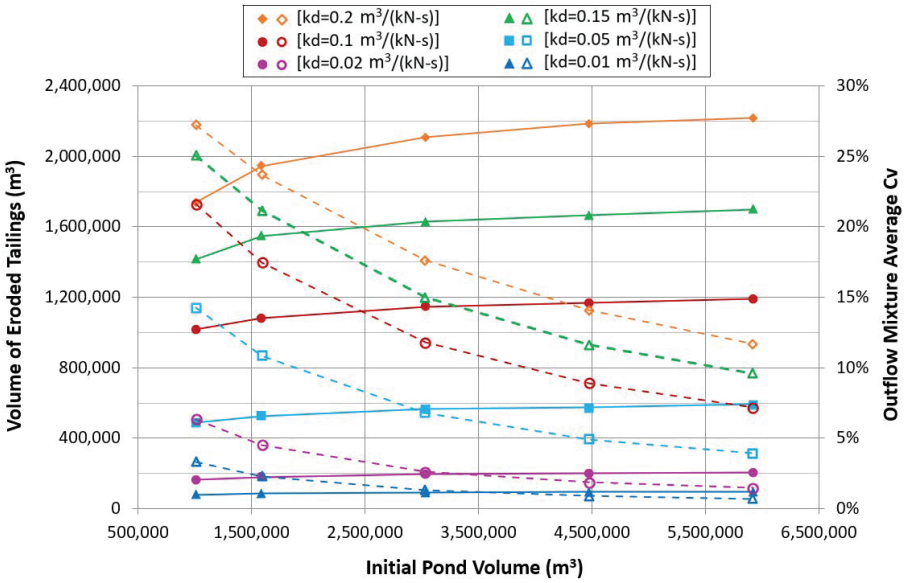

Figure 5: Parametric analysis of eroded tailings volume and average volumetric solids concentration of total outflow mixture of water and eroded tailings using probable range of erodibility coefficient and varied initial pond volume.

Observations from the parametric analysis results are summarized as follows.

With the same initial pond volume, the volume of eroded tailings increases with the increase of erodibility coefficient; the average volumetric solids concentration of the total outflow mixture also increases with the increase of erodibility coefficient.

With the same erodibility coefficient, the increase of initial pond volume slightly increases the volume of eroded tailings, but the average volumetric solids concentration of the total outflow mixture decreases.

When deposited tailings are less erodible and have relatively small erodibility coefficient, the eroded tailings volume has insignificant increment with the increase of initial pond volume.

For the range of parameters analyzed, the average volumetric solids concentration of the total outflow mixture of water and eroded tailings after hydraulic erosion does not exceed 30%. This is consistent with findings in studies of sediment/solids concentration in water floods which rarely exceeds 20% to 30% by volume (e.g. O'Brien 1986, García et al. 2008).

It is worth mentioning that the eroded tailings volume is not directly connected to storage volume of the deposited tailings in a storage facility. Geotechnical properties and integrity of the deposited tailings play a significant role in erodibility and influence the volume of eroded tailings.

The volume of eroded tailings shows logarithmical trend with the initial pond volume after the breach geometry is established, as summarized in Table 3.

$$\textit{Volume of Eroded Tailings} = \mathrm{A}\ \textit{ln}\ (\textit{Initial Pond Volume}) - \mathrm{B} \quad (5)$$

where A and B are the constants related to properties and integrity of the deposited tailings, and *ln* is denoted for *log* of base *e*.

Table 3. Relation between volume of eroded tailings and initial pond volume.

Erodibility coefficient (cm^3/N-s)	Erodibility coefficient (m^3/kN-s)	Relation between eroded tailings volume (y) and initial pond volume (x)
10	0.01	$y = 10622\ ln(x) - 67268$
20	0.02	$y = 23318\ ln(x) - 155573$
50	0.05	$y = 56743\ ln(x) - 290140$
100	0.1	$y = 96080\ ln(x) - 299523$
150	0.15	$y = 150170\ ln(x) - 628341$
200	0.2	$y = 266847\ ln(x) - 2000000$

* Logarithmical trend between volume of eroded tailings and initial pond volume was best fitted from results shown in Figure 5, where *ln* is denoted for *log* of base *e*.

5 CONCLUSION

In a tailings storage facility breach analysis the understanding of tailings hydraulic erosion characteristics and estimates of eroded tailings volume by pond water are essential when a supernatant pond exists and could be released. This paper proposed an erosion-based methodology and numerically simulated the hydraulic erosion process using MADflow, where tailings eroded and carried by discharge of supernatant pond were modelled as non-Newtonian fluids. The mixture of water and eroded tailings was simulated with varying solids concentration from the hydraulic erosion, and the resulting outflow hydrograph of water and eroded tailings mixture contains time-dependent solids concentration during the erosion process. The proposed methodology was validated with a flume experiment and the modelling results were found to be consistent with the experimental measurements.

The methodology was applied to a case study example with parametric analysis on erodibility coefficient and initial pond volume prior to hydraulic erosion of tailings. The analysis results show that the average volumetric solids concentration of total outflow mixture of water and eroded tailings does not exceed 30% for the probable range of parameters analyzed, which is consistent with typical findings in the studies of sediment/solids concentration in water floods. Furthermore, the eroded tailings volume is not directly connected to storage volume of deposited tailings. Geotechnical properties and integrity of the deposited tailings play a significant role in erodibility and influence the volume of eroded tailings. The volume of eroded tailings shows logarithmical trend with initial pond volume after breach geometry is established.

In-situ properties of deposited tailings in each tailings storage facility are unique. Taking site-specific conditions into consideration is recommended.

6 REFERENCES

Briaud, J.L., Govindasamy, A.V., and I. Shafii. 2017. Erosion Charts for Selected Geomaterials. *Journal of Geotechnical and Geoenvironmental Engineering*. 143(10): 04017072.

CDA (Canadian Dam Association). 2021. *Technical Bulletin - Tailings Dam Breach Analysis*.

Chen, H. and C.F. Lee. 2000. Numerical Simulation of Debris Flows. *Canadian Geotechnical Journal*, 37: 146-160.

Chen, H. and C.F. Lee. 2002. Runout Analysis of Slurry Flows with Bingham Model. *ASCE*, *Journal of Geotechnical and Geoenvironmental Engineering*, 128(12): 1032-1042.

Chen, H., Crosta, G.B., and C.F. Lee. 2006. Erosion Effect on Runout of Fast Landslides, Debris Flows and Avalanches: A Numerical Investigation. *Géotechnique*, 56(5): 305-322.

Chen, H. and D. Becker. 2014. Dam Breach Tailings Runout Analysis. *Canadian Dam Association Annual Conference*. Banff, Alberta. October 4-9, 2014.

Chen, H., Chin, B. and R. Friedel. 2019. Dam Breach Tailings Runout Modelling for Inactive/Closed Tailings Storage Facility. *Canadian Dam Association Annual Conference*. Calgary, Alberta. October 6-9, 2019.

Chen, H. and J. Cunning. 2021. Application of Critical State Soil Mechanics in Tailings Dam Breach Analysis. *Canadian Dam Association Annual Conference*. October 25-28, 2021.

Fontaine D.D. and V. Martin. 2015. Tailings Mobilization Estimates for Dam Breach Studies. *Proceedings of the 2015 Tailings and Mine Waste Conference*. Vancouver, BC, October 26-28, 2015.

García, M.H., R.C. MacArthur, R. French, and J. Miller. 2008. Sedimentation Hazards in Sedimentation Engineering edited by García, M.H. *ASCE Manuals and Reports on Engineering Practice* No. 110.

Ghahramani, N., Chen, H., Clohan, D., Liu, S., Llano, M., Rana, N., McDougall, S., Evans, S., and A. Take. 2022. A Benchmarking Study of Four Numerical Runout Models for the Simulation of Tailings Flows. *Science of the Total Environment*. 827 (154245). (https://doi.org/10.1016/j.scitotenv.2022.154245).

Hanson, G. J. 1989. Channel Erosion Study of Two Compacted Soils. *Transactions of the ASAE* 32(2): 485−490.

Hanson, G. J. 1990. Surface Erodibility of Earthen Channels at High Stresses Part II – Developing an In-Situ Testing Device. *Transactions of the ASAE*. 33(1): 132−137.

Hanson, G. J., and K. R. Cook. 2004. Apparatus, Test Procedures and Analytical Methods to Measure Soil Erodibility In-Situ. *Applied Engineering in Agriculture*. 20(4): 455-462.

Hanson, G.J., D.M. Temple, S.L. Hunt, and R.D. Tejral. 2011. Development and Characterization of Soil Material Parameters for Embankment Breach. *Applied Engineering in Agriculture*. 27(4): 587-595.

O'Brien, J.S. 1986. Physical Processes, Rheology, and Modeling of Mud Flows. *Ph.D. Dissertation*, Colorado State University, Fort Collins, Colorado.

Temple, D. M. 1985. Stability of Grass−Lined Channels Following Mowing. *Transactions of the ASAE*. 28(3): 750−754.

Wu, W. 2013. Simplified Physically Based Model of Earthen Embankment Breaching. *Journal of Hydraulic Engineering ASCE*. 139:837-851.